PHYSICAL REVIEW E **86**, 010101(R) (2012)

Thermal rectification in graded materials

Jiao Wang,[1] Emmanuel Pereira,[2] and Giulio Casati[3,4,5,*]

[1]*Department of Physics and Institute of Theoretical Physics and Astrophysics, Xiamen University, Xiamen 361005, China*

[2]*Departamento de Física-ICEx, UFMG, CP 702, 30.161-970 Belo Horizonte MG, Brazil*

[3]*Center for Nonlinear and Complex Systems, Università degli Studi dell'Insubria, Via Valleggio 11, 22100 Como, Italy*

[4]*Consorzio Nazionale Interuniversitario per le Scienze Fisiche della Materia, e CNR-INFM*

[5]*Istituto Nazionale di Fisica Nucleare, Sezione di Milano, via Celoria 16, 20133 Milano, Italy*

(Received 19 February 2012; published 3 July 2012)

In order to identify the basic conditions for thermal rectification we investigate a simple model with nonuniform, graded mass distribution. The existence of thermal rectification is theoretically predicted and numerically confirmed, suggesting that thermal rectification is a typical occurrence in graded systems, which are likely to be natural candidates for the actual fabrication of thermal diodes. In view of practical implications, the dependence of rectification on the asymmetry and system's size is studied.

DOI: 10.1103/PhysRevE.86.010101 PACS number(s): 44.10.+i, 05.40.−a, 05.60.Cd, 05.70.Ln

The study of the underlying dynamical mechanisms which determine the macroscopic properties of heat conduction has opened the fascinating possibility to control the heat current. In particular, a model of a thermal rectifier has been proposed [1] and since then, the phenomenon of thermal rectification has been intensively investigated [2–9] in order to analyze and improve the rectification effect, including experimental realizations [10].

However, as correctly pointed out in Ref. [3], most recurrent proposals of a thermal diode, based on the sequential coupling of two or three segments with different anharmonic potentials, are difficult to be experimentally implemented and the rectification power typically decays to zero with increasing the system size. In addition, most investigations so far have been based on numerical simulations and a much better theoretical understanding is highly desirable both for fundamental reasons as well as for obtaining useful hints for the actual realization of devices with satisfactory rectification power.

Along these lines, graded materials are attracting more and more interest: Papers with numerical [5–7], analytical [8,9] and even experimental [10] studies have appeared recently in the literature.

The present Rapid Communication addresses the fundamental dynamical mechanisms that lead to rectification. Our strategy is to consider a simple model that contains the minimal ingredients we theoretically judge to be necessary to rectification, and compare the numerical results with the theoretical predictions. As the features of our model are also shared by more realistic models such as anharmonic chains of oscillators, we conjecture that the obtained results may have practical implications as well. Our study allows us to understand the basic ingredients behind rectification, to describe nontrivial and important properties of the heat flow, and to show that rectification in graded materials could be a ubiquitous phenomenon.

We consider a chain [11] of elastically colliding particles of two kinds referred to, in the following, as "bars" and "bullets," respectively. (See Fig. 1.) Each bar is confined inside a cell of unit length; that is, besides elastic collisions with its neighboring bullet(s), it is also subject to elastic collisions with the two boundaries of the cell. A bullet only undergoes collisions with its two neighboring bars. Apart from collisions, all particles move freely. We denote the masses (velocities) of bars by M_l (v_l), $l = 1, \ldots, Z$, and those of bullets by m_k (u_k), $k = 1, \ldots, Z-1$, respectively, with Z being the total number of cells. Two statistical thermal baths with different temperatures τ_L and τ_R are put into contact with the two ends of the system: When the first (last) bar collides with the left (right) side of the first (last) cell, it is injected back with a new velocity determined by the distribution [12]

$$P_{L,R}(v) = \frac{|v|M_{1,Z}}{k_B\tau_{L,R}} \exp\left(-\frac{v^2 M_{1,Z}}{2k_B\tau_{L,R}}\right). \tag{1}$$

The Boltzmann constant k_B is set to be unity. In our molecular dynamics simulations, after the system reaches the steady state, we can compute the local temperature of each cell and the steady heat flux across the system. The local temperature of the lth cell is defined as the kinetic temperature of the bar, i.e., $\tau_l \equiv \langle M_l v_l^2/k_B\rangle$, where $\langle\cdot\rangle$ stands for the time average. The steady heat flux is measured as the time average of the energy exchanged in unit time between the left heat bath (the last bar) and the first bar (the right heat bath), or that between any two neighboring particles. We have verified that the so-measured heat flux is the same as the local heat flux carried by each particle, which is defined as $\langle M_l v_l^3/2\rangle$ ($\langle m_l u_l^3/2\rangle$) for the lth bar (bullet).

In order to investigate rectification, we consider the mass graded version of the above chain. Precisely, we will focus on a system with mass graded bullets $m_1 < m_2 < \cdots < m_{Z-1}$ and identical bars, $M_1 = \cdots = M_Z = 1$. In order to avoid boundary effects due to coupling with the heat baths, the rectification effects are measured numerically only over the N central cells, with the first (last) Z_L (Z_R) not being considered. Hence the effective system size is $N = Z - Z_L - Z_R$.

The starting point of our theoretical approach is the expression for the local heat flow inferred from the homogeneous case. We recall that the Fourier law of thermal conduction has been shown numerically to hold in the homogeneous version (i.e., the bullets also have the same mass $m_l = m$)

*giulio.casati@uninsubria.it

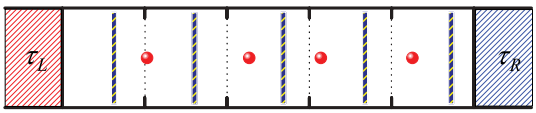

FIG. 1. (Color online) The schematic plot of our model. Dotted lines divide elementary unit cells. In each cell there is a bar which is subjected to elastic collisions with both cell boundaries and with neighboring bullets. The first (last) cell is coupled to a heat bath at temperature τ_L (τ_R).

of our model [11]. We also recall that homogeneous lattice models of oscillators with, e.g., quartic anharmonic on-site potentials, have been studied by different analytical methods [13–16] and shown to follow the Fourier law as well. It implies that for these systems, in the steady state the local heat current at position x is proportional to the temperature gradient $\mathcal{F}(x) = -\mathcal{K}(x)\nabla T(x)$, where the heat conductivity $\mathcal{K}(x)$ is a function of the local temperature $T(x)$ (and of other parameters). Precisely, for the homogeneous models of anharmonic oscillators, such a local expression reads

$$\mathcal{F} = (T_j - T_{j+1})/\mathcal{C}\bar{T}_j^{\beta}, \tag{2}$$

where T_j is the local temperature at the jth site and $\bar{T}_j^{\beta} = (T_j^{\beta} + T_{j+1}^{\beta})/2$ with $\beta \approx 2$. For the theoretical study of rectification in our inhomogeneous chain, we start from the inhomogeneous version of such equation, i.e., we write the heat flow from cell j to $j+1$ as

$$\mathcal{F}_{j,j+1} = -\mathcal{K}_j(\nabla T)_j = \frac{\left(\mathcal{C}_j T_j^{\alpha} + \mathcal{C}_{j+1} T_{j+1}^{\alpha}\right)}{2}(T_j - T_{j+1}). \tag{3}$$

Note that the homogeneous version of our model obeys the Fourier law with a thermal conductivity that scales as $T^{1/2}$ (see the following), in contrast to the $1/T^2$ behavior of the above anharmonic oscillators models.

For the heat flow in the steady state we have

$$\mathcal{F}_{1,2} = \mathcal{F}_{2,3} = \cdots = \mathcal{F}_{N-1,N} \equiv \mathcal{F}. \tag{4}$$

Hence, by summing up the $(N-1)$ equations in Eq. (3) for $j = 1,2,\ldots,N-1$, we get $\mathcal{F} = \mathcal{K}(T_1 - T_N)/(N-1)$, where

$$\mathcal{K} = \frac{(N-1)}{2}\left[\sum_{j=1}^{N-1}\frac{1}{\mathcal{C}_j T_j^{\alpha} + \mathcal{C}_{j+1} T_{j+1}^{\alpha}}\right]^{-1}. \tag{5}$$

Then the Fourier law follows in the case where the thermal conductivity $\mathcal{K}$ remains finite when $N \to \infty$.

From Eqs. (3) and (4), it follows that

$$\begin{aligned}(T_1 - T_2)\left(\mathcal{C}_1 T_1^{\alpha} + \mathcal{C}_2 T_2^{\alpha}\right) &= (T_2 - T_3)\left(\mathcal{C}_2 T_2^{\alpha} + \mathcal{C}_3 T_3^{\alpha}\right) \\ &= \cdots = (T_{N-1} - T_N)\left(\mathcal{C}_{N-1} T_{N-1}^{\alpha} \right. \\ &\quad \left. + \mathcal{C}_N T_N^{\alpha}\right).\end{aligned} \tag{6}$$

Thus, given the temperatures of the first and the last cell, i.e., T_1 and T_N, by using the equations above we may determine the inner temperatures $T_2, T_3, \ldots, T_{N-1}$. As it may be a hard problem to obtain the analytical solution of these equations, we may turn to numerical computations, or else, as in Refs. [8,9], we may assume small temperature gradients in order to simplify the computations. In this latter regime, i.e., for $T_1 = T + a_1\epsilon$, $T_N = T + a_N\epsilon$, ϵ small, we have $T_k = T + a_k\epsilon + O(\epsilon^2)$, where a_k have to be determined [we carry out the computations only up to $O(\epsilon)$]. Algebraic manipulations give us $a_k = a_1 + (a_N - a_1)\tilde{\mathcal{C}}(k)/\tilde{\mathcal{C}}(N)$, for $k = 2, \cdots, N-1$, where $\tilde{\mathcal{C}}(k) \equiv [(\mathcal{C}_1 + \mathcal{C}_2)^{-1} + (\mathcal{C}_2 + \mathcal{C}_3)^{-1} + \cdots + (\mathcal{C}_{k-1} + \mathcal{C}_k)^{-1}]$. The thermal conductivity defined in Eq. (5) is therefore

$$\mathcal{K} = \frac{(N-1)T^{\alpha}}{2}\left[\sum_{j=1}^{N-1}\left\{\frac{1}{(\mathcal{C}_j + \mathcal{C}_{j+1})} - \frac{\alpha\epsilon}{T}\frac{(a_j\mathcal{C}_j + a_{j+1}\mathcal{C}_{j+1})}{(\mathcal{C}_j + \mathcal{C}_{j+1})^2}\right\}\right]^{-1}. \tag{7}$$

Now we analyze the heat flow for the system with inverted thermal baths. In this case we denote the temperature of the jth cell by T_j' and assume that $T_1' = T_N$ and $T_N' = T_1$. We also write $T_k' = T + a_k'\epsilon$ for $k = 2,3,\ldots,N-1$, and after the computations we get $a_k' = a_N - (a_N - a_1)\tilde{\mathcal{C}}(k)/\tilde{\mathcal{C}}(N)$. Recalling that $a_1' = a_N$ and $a_N' = a_1$, one obtains for the thermal conductivity $\mathcal{K}'$ of the "inverted" system, an expression similar to $\mathcal{K}$ (with a_j' replacing a_j). We then have

$$\frac{1}{\mathcal{K}} - \frac{1}{\mathcal{K}'} = \frac{2\alpha(T_N - T_1)}{(N-1)T^{\alpha+1}\tilde{\mathcal{C}}(N)}\left\{\frac{(\mathcal{C}_1 - \mathcal{C}_2)}{(\mathcal{C}_1 + \mathcal{C}_2)^3} + \frac{(\mathcal{C}_2 - \mathcal{C}_3)}{(\mathcal{C}_2 + \mathcal{C}_3)^3} + \cdots + \frac{(\mathcal{C}_{N-1} - \mathcal{C}_N)}{(\mathcal{C}_{N-1} + \mathcal{C}_N)^3}\right\}. \tag{8}$$

The homogeneous model, where all bars have a unit mass and all bullets have mass m, has been shown [11] to follow the Fourier law and the thermal conductivity $\kappa(m,T)$ at temperature $T = 1$ is as shown in Fig. 2. As the dynamics of our model can be essentially described by a series of particle collisions, which is invariant under a time rescaling $t \to t/\gamma$ (with γ being a positive constant), or equivalently a temperature rescaling $T \to \sqrt{\gamma}T$, we have $\kappa(m,T) = \kappa(m,1)\sqrt{T}$. Therefore, in the limit of small temperature gradients, Eq. (3) leads to $\alpha = 1/2$.

To conclude our theoretical analysis we still have to determine the coefficients $\mathcal{C}_j$. The behavior of these coefficients as function of m can be deduced from Fig. 2 for the homogeneous chain. Indeed, let us also assume for our inhomogeneous system a small mass gradient and determine such coefficients by properly relating them to their homogeneous versions, i.e., $\mathcal{C}_j = [\kappa(m_{j+Z_L-1},1) + \kappa(m_{j+Z_L},1)]/2$.

The qualitative picture which now emerges is quite clear: From Eq. (8), in particular, from the difference between

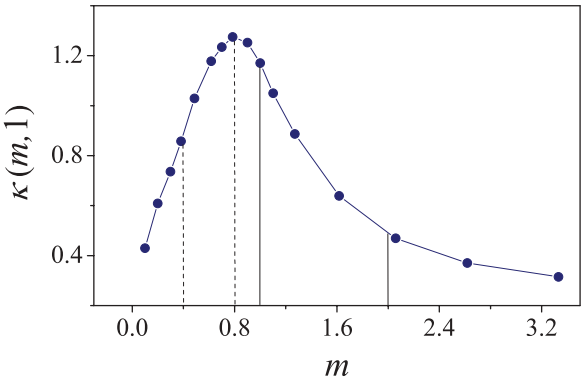

FIG. 2. (Color online) The numerically computed heat conductivity for the homogeneous chain of size $N = 45$ at temperature $T = 1$ (see Ref. [11]). The bars have unit mass and the bullets have the same mass m. The two solid (dotted) lines indicate the bullet mass region used for the simulations in Fig. 3(b) [Fig. 3(c)].

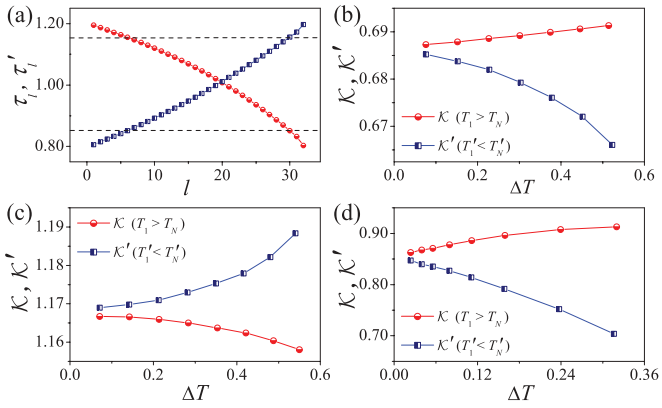

FIG. 3. (Color online) (a) Temperature profile of the graded chain with bullets' masses increasing in the interval (1,2) for $\tau_L = 1.2$ and $\tau_R = 0.8$ (red dots), and, inversely, $\tau'_L = 0.8$ and $\tau'_R = 1.2$ (blue squares). The dashed lines indicate the end temperatures T_1 (T'_N) and T_N (T'_1) of the central segment considered in our computations. (b)–(d) Heat conductivity measured over the central segment of the graded chain with (b) and (c) for bullets' masses increasing in the interval (1,2) and (0.4,0.8), respectively (all bars have unit mass), and (d) for the graded chain where all the masses of bars and bullets increase in the interval (1,2). See text for details.

the local thermal conductivities, we predict, and will later numerically confirm, the properties of rectification. First, from Eq. (8) it immediately follows the existence of rectification which is particularly clear when $\kappa(m_j,1)$, and so $\mathcal{C}_j$ has a monotonic behavior. It also follows that rectification increases with the gradient of temperature. Moreover, from Eq. (8), one can predict a larger flow from a smaller to larger mass direction in the region where $\kappa(m_j,1)$ decreases with m_j, and the opposite behavior in the region where $\kappa(m_j,1)$ increases with m_j. The fact that our approach allows to predict not only rectification of the heat current but also its direction is quite interesting. In this respect we recall that rectification in a graded system with the heat current larger in the direction of decreasing particle masses has been observed experimentally in nanotubes with nonhomogeneous external mass loading [10] and numerically in the mass graded Fermi-Pasta-Ulam model [5]. Instead, a case with the heat current larger in the reversed direction (of increasing masses) has been found by molecular dynamics simulations in mass graded ideal gases [6] and some carbon nanotubes [7].

We now turn to the molecular dynamics studies of our system which not only confirm our theoretical predictions but also extend, in fact, our analytical results to regimes beyond small gradients of temperature and mass, where the rectification phenomena become more relevant. To this end let us consider first a chain of $Z = 32$ cells with the bullets' masses increasing in the range (1,2) (i.e. the interval between the two solid vertical lines in Fig. 2) with $m_l = 1 + l/Z$. After the steady state is reached we calculate the time averaged temperature profile and the heat current. Averages are taken over a number of collisions per particle larger than 2×10^9. In Fig. 3(a) we show the computed temperature profile for $\tau_L = 1.2$ and $\tau_R = 0.8$, as well as for $\tau'_L = 0.8$ and $\tau'_R = 1.2$. To evaluate the heat conductivity $\mathcal{K}$ and $\mathcal{K}'$ we neglect the first (last) Z_L (Z_R) cells in order to get rid of the boundary effects. The values of Z_L and Z_R are determined by ensuring that $T_1 = T'_N$ and $T_N = T'_1$. (Note that $T_l = \tau_{l+Z_L}$ and $T'_l = \tau'_{l+Z_L}$ for $l = 1,\ldots,N$.) In this case we have $Z_L = 5$ and $Z_R = 2$. [See Fig. 3(a).] The value of thermal conductivity $\mathcal{K} = \mathcal{F}(N-1)/(T_1 - T_N)$ is then calculated over the central segment of $N = 25$ cells with numerically measured $\mathcal{F}$, T_1, and T_N. $\mathcal{K}'$ is computed in the same way.

The dependence of the heat conductivity $\mathcal{K}$ and $\mathcal{K}'$ on ΔT for $T = 1$ is given in Fig. 3(b). Here $T_1 = T'_N = T + \Delta T$ and $T_N = T'_1 = T - \Delta T$. It is clearly seen that a system with graded mass particles does present rectification, and that rectification increases with the temperature gradient. In addition, as in this case C_j decreases monotonically (see the region between two solid vertical lines in Fig. 2), according to our theoretical analysis the value of $\mathcal{K}$ for $T_1 > T_N$ should be larger than $\mathcal{K}'$ for $T'_1 < T'_N$. This is confirmed by the numerical results.

One advantage of our model is that, as shown in Fig. 2, it can display regions where C_j decreases with j as well as regions where C_j increases with j as, e.g., in the interval between the two dashed vertical lines in Fig. 2. In the latter situation we predict that the behavior of $\mathcal{K}$ and $\mathcal{K}'$ will be opposite to the previous case, i.e., that $\mathcal{K}$ for $T_1 > T_N$ will be smaller than $\mathcal{K}'$ for $T'_1 < T'_N$. This is confirmed by Fig. 3(c) where we present the numerical results for a graded chain with the masses of bullets in the interval (0.4,0.8) with $m_l = 0.4(1 + l/Z)$. All the computations are done as before with $Z = 32$, $Z_L = 3$, $Z_R = 4$, $N = 25$, and $T = 1$.

An obvious interesting question is how to enhance rectification in our graded chain. As our theoretical analysis suggests, a possible way to increase rectification is to increase the asymmetry of the system. We have therefore analyzed the case where the masses of the bars are also allowed to have a graded distribution. To be precise, all the masses are graded in between 1 and 2. Namely, $M_l = 1 + (l - 0.5)/Z$ for $l = 1,\ldots,Z$ and $m_l = 1 + l/Z$ for $l = 1,\ldots,Z-1$. Here we take $Z = 32$, $Z_L = 5$, $Z_R = 1$, $N = 26$, and $T = 1$. The results are depicted in Fig. 3(d) and show a significant increase in rectification. We stress that the increase of rectification with asymmetry is an important effect which may be of practical

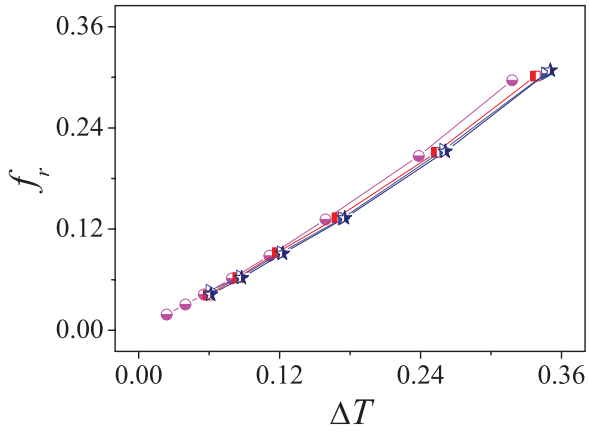

FIG. 4. (Color online) The rectification measured over the central segment of the graded chain where all the masses of bars and bullets increase linearly in the interval (1,2). The dots, squares, triangles, and stars represent the results for system size $Z = 32$, 64, 128, and 256, respectively.

interest: Similar mechanisms may be present in more realistic models due to graded interparticle interactions and/or graded on-site potentials, in addition to graded masses.

Finally, we remark that for the case presented in Fig. 3(d) the heat conductivity $\mathcal{K}$ and $\mathcal{K}'$ essentially do not change with the system size. This has been verified by additional simulations with $Z = 64$, 128, and 256 (with $Z_L = 8$, 15, and 29, $Z_R = 2$, 4, and 8, and $N = 54$, 109, and 229, respectively). The rectification, defined as $f_r \equiv (\mathcal{K} - \mathcal{K}')/\mathcal{K}'$, does not change with the system size, as clearly illustrated in Fig. 4. The fact that rectification does not vanish with increasing the system size is an important property, which is absent in the known diode models given by the sequential coupling of different segments.

In summary, in this work, we have performed analytical and numerical investigations of the heat flow in a simple model, devoid of intricate interactions, in order to find results of general validity. Our results demonstrate that thermal rectification takes place in asymmetric systems with local heat flow proportional to the temperature gradient and with the local conductivity depending on temperature. This conclusion is also supported by additional numerical investigations [17], along the lines of Refs. [11] and [18], of the energy diffusive behavior and of correlation properties of energy fluctuations. Finally, it is interesting to notice that in our model the diffusive behavior (typical of the Fourier law) is associated with the thermal rectification phenomenon.

J.W. is supported by the NNSF (Grant No. 10975115) and SRFDP (Grant No. 20100121110021) of China, E.P. by CNPq (Brazil), and G.C. by the MIUR-PRIN 2008 and by Regione Lombardia.

[1] M. Terraneo, M. Peyrard, and G. Casati, Phys. Rev. Lett. **88**, 094302 (2002).
[2] B. Li, L. Wang, and G. Casati, Phys. Rev. Lett. **93**, 184301 (2004).
[3] B. Hu, L. Yang, and Y. Zhang, Phys. Rev. Lett. **97**, 124302 (2006).
[4] B. Li, L. Wang, and G. Casati, Appl. Phys. Lett. **88**, 143501 (2006).
[5] N. Yang, N. Li, L. Wang, and B. Li, Phys. Rev. B **76**, 020301(R) (2007).
[6] H.-B. Li, Q.-M. Nie, and X.-T. Xin, Chin. Phys. Lett. **26**, 074401 (2009).
[7] M. Alaghemandi, E. Algaer, M. C. Böhm, and F. Müller-Plathe, Nanotechnology **20**, 115704 (2009); M. Alaghemandi, F. Leroy, F. Müller-Plathe, and M. C. Böhm, Phys. Rev. B **81**, 125410 (2010).
[8] E. Pereira, Phys. Rev. E **82**, 040101(R) (2010).
[9] E. Pereira, Phys. Rev. E **83**, 031106 (2011).
[10] C. W. Chang, D. Okawa, A. Majumdar, and A. Zettl, Science **314**, 1121 (2006); W. Kobayashi, Y. Teraoka, and I. Terasaki, J. Electron. Mater. **39**, 1488 (2010)
[11] B. Li, G. Casati, J. Wang, and T. Prosen, Phys. Rev. Lett. **92**, 254301 (2004).
[12] J. L. Lebowitz and H. Spohn, J. Stat. Phys. **19**, 633 (1978); R. Tehver, F. Toigo, J. Koplik, and J. R. Banavar, Phys. Rev. E **57**, R17 (1998).
[13] J. Bricmont and A. Kupiainen, Phys. Rev. Lett. **98**, 214301 (2007); Commun. Math. Phys. **274**, 555 (2007).
[14] K. Aoki, J. Lukkarinen, and H. Spohn, J. Stat. Phys. **124**, 1105 (2006).
[15] K. Aoki and D. Kusnezov, Phys. Lett. A **265**, 250 (2000).
[16] N. Li and B. Li, Phys. Rev. E **76**, 011108 (2007).
[17] J. Wang, E. Pereira, and G. Casati (unpublished).
[18] H. Zhao, Phys. Rev. Lett. **96**, 140602 (2006).